REPORT DOCUMENTATION PAGE

Form Approved
OMB No. 0704-0188

1. REPORT DATE *(DD-MM-YYYY)*	2. REPORT TYPE	3. DATES COVERED *(From - To)*
31-10-2003		

4. TITLE AND SUBTITLE
Influence of Wavelength on the Parameterization of Drag Coefficeient and Surface Roughness

5a. CONTRACT NUMBER

5b. GRANT NUMBER

5c. PROGRAM ELEMENT NUMBER
0601153N

6. AUTHOR(S)
Paul A. Hwang

5d. PROJECT NUMBER

5e. TASK NUMBER

5f. WORK UNIT NUMBER
73-8190-03-5

7. PERFORMING ORGANIZATION NAME(S) AND ADDRESS(ES)
Naval Research Laboratory
Oceanography Division
Stennis Space Center, MS 39529-5004

8. PERFORMING ORGANIZATION REPORT NUMBER
NRL/JA/7330-03-6

9. SPONSORING/MONITORING AGENCY NAME(S) AND ADDRESS(ES)
Office of Naval Research
800 N. Quincy St.
Arlington, VA 22217-5660

10. SPONSOR/MONITOR'S ACRONYM(S)
ONR

11. SPONSOR/MONITOR'S REPORT NUMBER(S)

12. DISTRIBUTION/AVAILABILITY STATEMENT
Approved for public release, distribution is unlimited.

13. SUPPLEMENTARY NOTES

14. ABSTRACT
Surface waves are the roughness element of the ocean surface, the air-sea interaction processes are influenced by the wave conditions. The dynamic influence of surface waves decays exponentially with distance from the air-water interface. The relevant length scale characterizing the decay rate is the wavelength. The parameterization of drag coefficient and surface roughness can be significantly improved by using wavelength as the reference length scale of atmospheric measurements. The wavelength scaling of drag coefficient and dynamic roughness also receives support from theoretical studies of wind and wave coupling.

15. SUBJECT TERMS
drag coefficient, surface roughness, parameterization, wavelength, fetch limited, wind stress

16. SECURITY CLASSIFICATION OF:			17. LIMITATION OF ABSTRACT	18. NUMBER OF PAGES	19a. NAME OF RESPONSIBLE PERSON
a. REPORT	b. ABSTRACT	c. THIS PAGE			Paul A. Hwang
Unclassified	Unclassified	Unclassified	SAR	7	19b. TELEPHONE NUMBER *(Include area code)* 228-688-4708

Journal of Oceanography, Vol. 60, pp. 835 to 841, 2004

Influence of Wavelength on the Parameterization of Drag Coefficient and Surface Roughness

PAUL A. HWANG*

Oceanography Division, Naval Research Laboratory, Stennis Space Center, MS 39529-5004, U.S.A.

(Received 1 July 2003; in revised form 19 October 2003; accepted 31 October 2003)

Surface waves are the roughness element of the ocean surface, the air-sea interaction processes are influenced by the wave conditions. The dynamic influence of surface waves decays exponentially with distance from the air-water interface. The relevant length scale characterizing the decay rate is the wavelength. The parameterization of drag coefficient and surface roughness can be significantly improved by using wavelength as the reference length scale of atmospheric measurements. The wavelength scaling of drag coefficient and dynamic roughness also receives support from theoretical studies of wind and wave coupling.

Keywords:
· Drag coefficient,
· surface roughness,
· parameterization,
· wavelength,
· fetch limited,
· wind stress.

1. Introduction

Drag coefficient (C_D) and surface roughness (z_0) are important parameters for quantifying air-sea momentum and energy exchanges. For a long time the drag coefficient of the ocean surface has been considered a constant (e.g., Kraus, 1972). As the quality and quantity of measurements have improved, it has become evident that drag coefficient tends to increase with increasing wind speed (e.g., Garratt, 1977; Wu, 1980). Later, it was found that in addition to wind speed, stability stratification, sea state and wave conditions are also important in modifying the drag coefficient (e.g., Donelan, 1982, 1990; Toba *et al.*, 1990; Jones and Toba, 2001). The study of drag coefficient can also be approached by investigating the surface roughness parameter, frequently expressed in the dimensionless form $z_{0*} = gz_0/u_*^2$, where g is the gravitational acceleration and u_* is the wind friction velocity. The dimensionless roughness z_{0*} is generally referred to as the Charnock parameter and was originally considered a constant (e.g., Charnock, 1955; Wu, 1980). Later on, more extensive measurements have convincingly illustrated that z_{0*} does not remain constant and there seems to be good correlation between z_{0*} and surface wave properties such as wave height and wave slope (e.g., Donelan, 1990; Donelan *et al.*, 1993; Anctil and Donelan, 1996; Taylor and Yelland, 2001) or wave period (e.g., Toba *et al.*, 1990).

Over many decades of intensive research, our knowledge of the stability correction has advanced significantly (e.g., Garratt, 1977; Donelan, 1990; Geernaert, 1999; Toba *et al.*, 2001). In contrast, a consistent parameterization of C_D with wave parameters remains elusive. Some earlier works have introduced wave height or wavelength into the parameterization of drag coefficient and surface roughness (e.g., Kitaigorodskii, 1973; Stewart, 1974; Donelan, 1990). Recently, Makin and Kudryavtsev (1999, 2002) and Makin (2003) developed wind-over-wave coupling (WOWC) theory, focusing on the dynamics of microscale air-sea interactions. The surface wind stress has been shown to be significantly influenced by the surface wave dynamics through the form drag, which is the correlation of wave-induced pressure field and the surface wave slope. The form drag is further divided into a non-separated sheltering component and the stress due to flow separation from breaking of both small-scale and dominant-scale waves. Numerical computations have been carried out to demonstrate the relative importance of the different surface stress components and their dependence on wind speed, wave age, finite water depth and other atmospheric and wave parameters. In the WOWC analysis, the wavelength at the spectral peak is a clear scaling length of air-sea interaction processes.

Almost all the earlier analyses of C_D and z_0 use the reference wind speed at 10 m elevation (U_{10}). Although the employment of U_{10} in the analyses provides a consistent reference level of wind measurements (as compared to earlier reports using "mast height" or "anemometer height"), the dynamical significance of the 10-m elevation in the marine boundary layer is not clear. From a heuristic point of view, surface waves are the ocean surface roughness, the air-sea interaction processes are influenced by the wave conditions. Because the influence

* E-mail address: paul.hwang@nrlssc.navy.mil

of surface waves decays exponentially with the wavelength serving as the vertical length scale, the dynamically meaningful reference elevation should be the characteristic wavelength of the peak component of surface wave spectrum, λ. As described in the last paragraph, this common sense vertical length scale also receives theoretical support from the study of wind over waves coupling. This paper presents an analysis with $U_{\lambda/2}$ serving as the reference wind speed, where $U_{\lambda/2}$ is the wind speed at the elevation equal to one-half of the surface wavelength. The general conclusions of this paper are not changed by using different fractions of the wavelength as the vertical length scale of wind speed reference; more discussions on this point will be presented later. The functional expressions of the drag coefficient referenced to $U_{\lambda/2}$ (expressed as $C_{\lambda/2}$ to distinguish it from C_{10}, the drag coefficient referenced to U_{10}) and surface roughness and their dependence on the wind and wave parameters are described. The dimensionless roughness in the form of $k_p z_0$ falls out naturally when wavelength is used as the reference length scale, where $k_p = 2\pi/\lambda$ is the wavenumber at the spectral peak. The relation between $k_p z_0$ and z_{0*} can be easily derived.

The detail of the analysis with $U_{\lambda/2}$ as the reference wind speed and the parameterization of surface roughness in terms of $k_p z_0$ and z_{0*} is given in Section 2. Field data with wind stress measurements under conditions dominated by wind seas are assembled to verify the results obtained from the analysis (Section 3). A comparison of $C_{\lambda/2}$ and C_{10} illustrates the superiority of the former for grouping together datasets from different sources. Similarly, the dimensionless roughness represented by $k_p z_0$ consolidates data better than z_{0*}. Section 4 presents discussions on the issue of possible spurious correlation when scaling with u_* (Smith *et al.*, 1992) in the parameterization function of the drag coefficient and surface roughness. The analysis indicates that spurious correlation does not pose a problem in the datasets used in the present study. The summary and conclusions are given in Section 5.

2. Analysis

In this paper, the discussion is limited to neutral stratification or to the situation that the stability correction has been performed. The vertical wind speed distribution is described by the logarithmic wind profile,

$$U(z) = \frac{u_*}{\kappa} \ln \frac{z}{z_0}, \tag{1}$$

where U is the equivalent wind speed at neutral condition, κ is the von Kármán constant (0.4), and z is the vertical elevation measured from the mean water surface. Taking the reference length scale for wind speed measurements at the level equal to one-half of the wavelength, the drag coefficient $C_{\lambda/2} = u_*^2/U_{\lambda/2}^2$ can be written as

$$C_{\lambda/2} = \kappa^2 \left(\ln \frac{\pi}{k_p z_0} \right)^{-2}. \tag{2}$$

The approach of using k_p for the characteristic wave component is expected to work well in wind-sea dominated wave conditions. The influence of swell on the drag coefficient and surface roughness requires further investigation.

Equation (2) suggests that a natural expression of the dimensionless surface roughness is $k_p z_0$, and from (2)

$$k_p z_0 = \pi \exp\left(-\kappa C_{\lambda/2}^{-0.5}\right). \tag{3}$$

Using the dispersion relation of surface waves,

$$\omega_p^2 = g k_p \tanh k_p h, \tag{4}$$

$k_p z_0$ can appear in several different forms

$$k_p z_0 = z_{0*} \left(\frac{u_*}{C_p} \right)^2 \tanh k_p h = z_{0*} \left(\frac{U_{\lambda/2}}{C_p} \right)^2 C_{\lambda/2} \tanh k_p h$$
$$= \frac{z_{0*} \omega_{**}^2}{\tanh k_p h} = \frac{z_{0*} \omega_*^2 C_{\lambda/2}}{\tanh k_p h}, \tag{5}$$

where $\omega_{**} = u_* \omega_p / g$ and $\omega_* = U_{\lambda/2} \omega_p / g$, both can be interpreted as the dimensionless frequency of the air-sea coupled system; ω_p and C_p are the angular frequency and phase speed, respectively, of the peak spectral component. For deep water, the dimensionless frequency is identical to the inverse wave age u_*/C_p or $U_{\lambda/2}/C_p$.

The analysis of the logarithmic wind profile leads to one equation (Eq. (2) or (3)) connecting two dimensionless unknowns ($C_{\lambda/2}$ and $k_p z_0$). To make further progress, either another wind-wave coupling function or assumption needs to be introduced or an empirical relation of $C_{\lambda/2}$ or $k_p z_0$ needs to be established. The next section presents an analysis of results from several field experiments (Donelan, 1979; Merzi and Graf, 1985; Anctil and Donelan, 1996; Janssen, 1997). The selected datasets are characterized by wind-sea dominated wave conditions and the tabulated data list sufficient information on wave properties and water depth to derive the wavelength. The investigation shows that among the dependence of $C_{\lambda/2}$, $k_p z_0$ and z_{0*} on u_*/C_p, $U_{\lambda/2}/C_p$, ω_{**} or ω_*, the

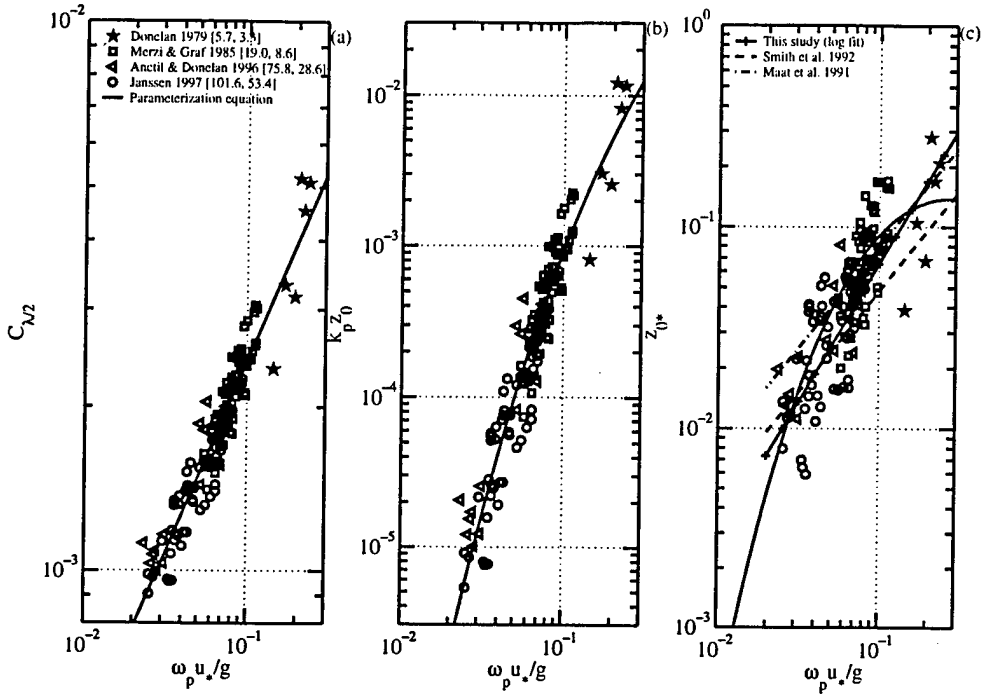

Fig. 1. (a) Drag coefficient $C_{\lambda/2}(\omega_{**})$ measured in wind-sea dominated wave conditions. The numbers within the square brackets in the legends are the maximum and minimum wavelengths in each individual dataset; the curve represents the parameterization equation (6). (b) Dimensionless roughness in terms of $k_p z_0(\omega_{**})$, the curve represents the parameterization equation (7). (c) Dimensionless roughness in terms of $z_{0*}(\omega_{**})$, the curve represents the parameterization equation (8). (c) also shows the curve from least square power-law fitting of $z_{0*}(C_p/u_*)$. The functions given by Maat *et al.* (1991) and Smith *et al.* (1992) are also illustrated (Section 4) for comparison.

parameterization of $C_{\lambda/2}(\omega_{**})$ yields a simple power-law function,

$$C_{\lambda/2} = A_c \omega_{**}^{a_c}, \tag{6}$$

where $A_c = 1.22 \times 10^{-2}$ and $a_c = 0.704$. More details of the analysis of the field data are presented in the next section. The dimensionless roughness becomes

$$k_p z_0 = \pi \exp\left[-\kappa\left(A_c \omega_{**}^{a_c}\right)^{-0.5}\right]. \tag{7}$$

The dimensionless roughness expressed as the Charnock coefficient can be obtained from substitution of (5) in (7),

$$z_{0*} = \pi \tanh kh\, \omega_{**}^{-2} \exp\left[-\kappa\left(A_c \omega_{**}^{a_c}\right)^{-0.5}\right]. \tag{8}$$

Other expressions of the dimensionless roughness in terms of u_*/C_p or $U_{\lambda/2}/C_p$ can also be constructed and will not be further elaborated here.

3. Comparison with Field Measurements

In order to verify the analysis presented in the last section, tabulated field data reported by Donelan (1979), Merzi and Graf (1985), Anctil and Donelan (1996) and Janssen (1997) have been assembled. All these datasets share several common attributes, including data quality control screening for steady wind events, fetch-limited wave conditions, direct wind stress measurements using either the profile method or the eddy correlation technique, and they contain sufficient information to derive the peak wavelength. The listed wind velocity is corrected for the stability influences. Moreover, most of the data have been collected in finite-depth waters; therefore, a proper accounting of the depth effect as described in (5) or (8) should be applied when the Charnock parameter is used for the dimensionless surface roughness. However, the data scatter is rather large, the depth effect is masked and the scatter plots of $z_{0*}(\omega_{**})$ and $z_{0*}/\tanh(kh)(\omega_{**})$ are not very different (not shown). A brief description of these experiments is given in Appendix A.

Figure 1(a) displays the dependence of $C_{\lambda/2}$ on ω_{**} processed from the assembled data. Although the data scatter is large, the result is a substantial improvement

over the expressions of C_{10}. Figure A1 in Appendix A shows several presentations of C_{10}, including (a) $C_{10}(U_{10})$, (b) $C_{10}(\omega_{**})$, and (c) $C_{10}(U_{10}/C_p)$. The C_{10} representations result in sets of curves and clearly require a secondary parameter. Comparing the results presented in Figs. 1 and A1, it is obvious that $C_{\lambda/2}(\omega_{**})$ does indeed provide a better parameterization than C_{10} regarding the surface wave effects on the drag coefficient. Polynomial fitting of a power law function to the combined data presented in Fig. 1(a) yields the empirical function of $C_{\lambda/2}(\omega_{**})$ given in (6). (Different parameterizations of $C_{\lambda/2}$ with u_*/C_p and other combinations of wind and wave parameters have also been investigated. For example, the regression constant and exponent for u_*/C_p parameterization are 1.09×10^{-2} and 0.696, respectively. The root mean square (rms) difference between the regression curve and the measurements is 2.78×10^{-4}, which is about 20 percent larger than $C_{\lambda/2}(\omega_{**})$ parameterization with an rms difference of 2.26×10^{-4}.) The issue of the fraction of wavelength as the vertical reference level is also studied. Examples of using $U_{\lambda/4}$, $U_{\lambda/6}$, $U_{\lambda/8}$ as reference wind speeds are given in Appendix B, showing that the wavelength scaling of the drag coefficient is not influenced by the choice of the proportionality constant.

The dimensionless roughness $k_p z_0(\omega_{**})$ is shown in Fig. 1(b). The measured data again display a smooth variation with ω_{**} and measurements from different sources collapse very well following the proposed parameterization function (7), given as the solid curve in the figure. In terms of the Charnock parameter, z_{0*} (Fig. 1(c)), the dimensionless roughness increases with ω_{**} in the parameter range of the available data. The parameterization function (8) predicts that the dependence of $z_{0*}(\omega_{**})$ reverses to a decreasing trend at $\omega_{**} > \sim 0.25$ and z_{0*} approaches ω_{**}^{-2} asymptotically as $\omega_{**} \to \infty$. Field data at very high ω_{**} are difficult to obtain so such non-monotonic behavior cannot be positively confirmed from the field measurements assembled here. The inverse relationship of $z_{0*}(\omega_{**})$ at high ω_{**} range has been observed in laboratory measurements (e.g., Toba *et al.*, 1990).

4. Discussions

From the point of view of dimensional analysis, (6) can be interpreted as choosing peak wavelength and phase velocity of surface waves as the length and velocity scales for organizing the observations. As discussed earlier, these scaling factors are logical choices because the roughness of the ocean surface is primarily composed of surface waves. Moreover, the study of wind over wave coupling supports the suggestion of peak wavelength as the vertical scaling length for parameterizations (Makin and Kudryavtsev, 1999, 2002; Makin, 2003).

Smith *et al.* (1992) caution about the possible hazards of self-correlation in scaling with u_* because the exponential dependence of z_0 on u_* (and that wind speeds at different elevations—e.g., from instrument height to $z = 10$ m or $\lambda/2$—are subsequently computed from z_0 and u_* using the function describing the wind speed profile). They provide two test criteria for determining whether the spurious correlation is negligible in a dataset (p. 134, *ibid.*) with $z_{0*} \sim (C_p/u_*)^a$,

$$\text{var}(\ln Z) << \text{var}(\ln Y), \text{ and } \text{var}(\ln W) << \text{var}(\ln X), \quad (9)$$

where $Z = u^a$, $Y = (gz/u_*^2)\exp(-\kappa U/u_*)u_*^a$, $W = u_*$, $X = C_p$ and the function var is the variance of the argument in parentheses. They further comment that the second condition is usually not met in most field data (in the example cited by them, the four variances are $\text{var}(\ln Z) = 0.146$, $\text{var}(\ln Y) = 0.486$, $\text{var}(\ln W) = 0.146$, and $\text{var}(\ln X) = 0.0057$), thus "the variability of $\ln u_*$ is not smaller than that of $\ln C_p$, variation of $\ln(C_p/u_*)$ is due more to u_* than to C_p, and self-correlation has influenced the fit to obtain (the parameterization equation)." They further comment that "This does not disprove (the parameterized equation) ..." and that "As far as we know, other similar data sets would lead to the same impasse if tested for spuriousness."

The four datasets assembled in this paper cover a considerably wider range of wind sea conditions. The least square fitting of the combined data yields $z_{0*} = 1.50(C_p/u_*)^{-1.36}$. The fitted power-law function is shown in Fig. 1(c) in terms of $z_{0*}(\omega_{**})$, where $C_p/u_* = \omega_{**}^{-1}$ for deep water condition. As noted earlier, the large data scatter has masked the depth effect in these datasets. For comparison, the functions presented by Maat *et al.* (1991) and Smith *et al.* (1992), $z_{0*} = 0.8(C_p/u_*)^{-1}$ and $z_{0*} = 0.48(C_p/u_*)^{-1}$, respectively, are also illustrated. The computed variances are $\text{var}(\ln Z) = 0.278$, $\text{var}(\ln Y) = 0.687$, $\text{var}(\ln W) = 0.150$, and $\text{var}(\ln X) = 0.202$. The problem of spurious self-correlation is not expected to be serious in the present analysis.

5. Summary and Conclusions

The dynamic influence of surface waves decays exponentially with distance from the air-water interface and the decay rate is inversely proportional to the characteristic wavelength. These dynamic properties of surface waves suggest that the reference wind speed for atmospheric measurements on air-sea coupling parameters should be the wind speed at an elevation proportional to the wavelength. The wavelength scaling also receives strong support from wind over wave coupling theory (e.g., Makin and Kudryavtsev, 1999, 2002; Makin, 2003). The analytical expressions of the drag coefficient and surface roughness with $U_{\lambda/2}$ as reference wind speed are established from the logarithmic wind profile (Section 2) for

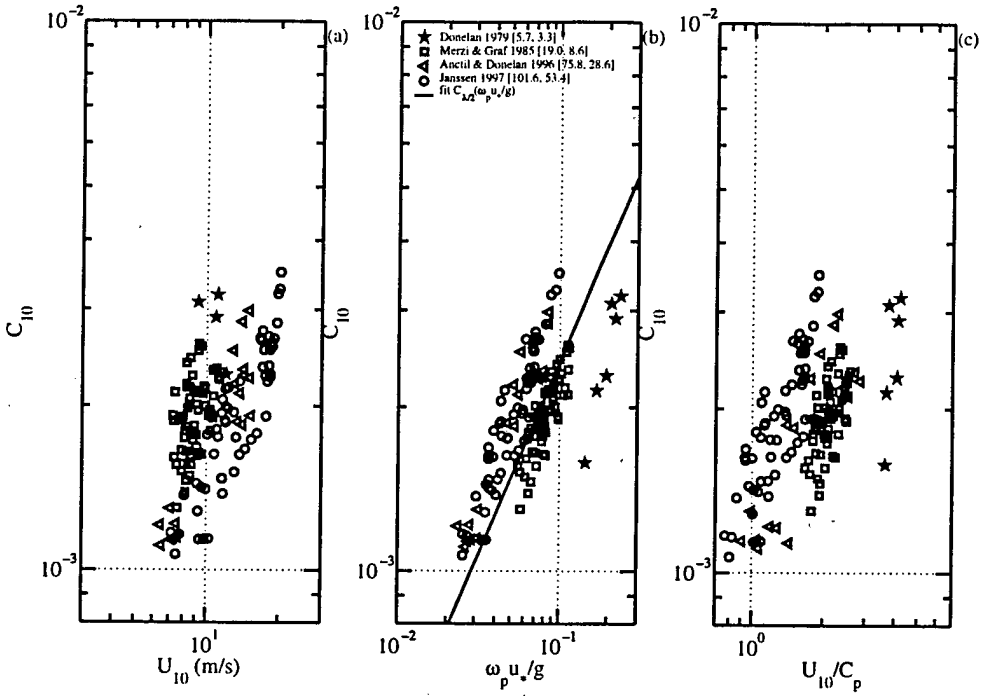

Fig. A1. Drag coefficient in terms of C_{10} presented as (a) $C_{10}(U_{10})$, (b) $C_{10}(\omega_{**})$, and (c) $C_{10}(U_{10}/C_p)$. The data scatter in these expressions is considerably worse than the $C_{\lambda/2}(\omega_{**})$ expression shown in Fig. 1(a) and suggests the necessity of a secondary parameter for C_{10}.

stratification-corrected conditions and wind-sea dominated wave fields. The analysis suggests that a natural expression of the dimensionless surface roughness is $k_p z_0$. Other expressions of the nondimensional surface roughness, such as the Charnock parameter, can be obtained by the substitution of k_p with ω_p using the dispersion relation of surface gravity waves.

Several field experiments with wind-sea dominated wave fields and tabulated data that provide sufficient information to derive wavelengths have been analyzed. The results show that the measurements of the drag coefficient from different experiments can be consolidated in a more organized manner when it is presented in terms of $C_{\lambda/2}$ than in terms of C_{10} (compare Figs. 1(a) and A1). With the consideration that wavelength and wave phase speed are the proper length and velocity scales of the ocean surface roughness, the parameterization of $C_{\lambda/2}(\omega_{**})$ is given by an empirical power-law function (6). The dimensionless roughness can then be represented by (7) for $k_p z_0(\omega_{**})$ or by (8) for $z_{0*}(\omega_{**})$. Surface roughness in terms of $k_p z_0$ increases monotonically with ω_{**}. When expressed in terms of z_{0*} the roughness increases with ω_{**} for $\omega_{**} < \sim 0.25$ and decreases with ω_{**} for $\omega_{**} > \sim 0.25$. The range of ω_{**} in the field data is usually much less than 0.25 but laboratory data extend to a much higher ω_{**} range (e.g., Toba *et al.*, 1990).

Acknowledgements

This work is sponsored by the Office of Naval Research (Naval Research Laboratory PE61153N). Nancy Mangin assisted in data assemby and manuscript preparation (NRL Contribution NRL/JA/7330-03-0006).

Appendix A. Descriptions of the Assembled Datasets

Donelan (1979) acquires wind and wave measurements from a fixed tower at the western side of Lake Ontario. The tower is located 1100 m from the coast, and the local water depth is 12 m. An extensive suite of instruments are mounted on the tower. Data relevant to this study include wind velocity, direct wind stress measurement using the eddy correlation method, wave variance and peak frequency of the wave spectrum. The wind conditions selected for his analysis are steady offshore blowing events with directions of both winds and waves staying within 25 degrees to the beach normal, and that the peak frequency of a companion waverider buoy deployed further offshore to be less than 3.14 rad/s. All together, six cases are reported. The maximum and minimum wavelengths in this dataset are 5.7 and 3.3 m.

Merzi and Graf (1985) conduct wind stress measurements in Lake Geneva. The measurement station is on the northern part of the lake. The local water depth is 3 m. The records selected for analysis are based on steady

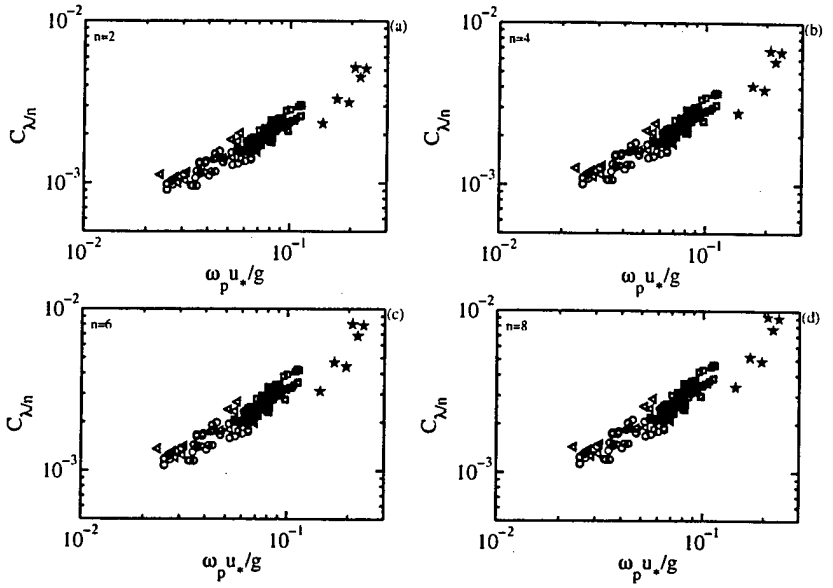

Fig. B1. Comparison of (a) $C_{\lambda/2}(\omega_{**})$, (b) $C_{\lambda/4}(\omega_{**})$, (c) $C_{\lambda/6}(\omega_{**})$, and (d) $C_{\lambda/8}(\omega_{**})$. The wavelength scaling for the drag coefficient is not qualitatively influenced by the choice of the proportionality constant.

southwesterly events and well-behaved wind profiles (60 cases). The friction velocity is derived from the profile method. Thermal stratification is corrected. The friction velocity used in this analysis is calculated from their tabulated neutral drag coefficient and U_{10}. The maximum and minimum wavelengths in this dataset are 19.0 and 8.6 m.

Anctil and Donelan (1996) report momentum flux observations from four towers at different depths along a shore-normal line at the west end of Lake Ontario, Canada. The nominal depths of the towers are 2, 4, 8, and 12 m, the wind stress is measured by the eddy correlation method at anemometer heights of 6.2, 7.8, 7.4 and 12 m for the four towers. The drag coefficients and wind speeds at both anemometer heights and 10 m reference elevation are tabulated along with the stability parameter, instantaneous water depth, root mean square wave height, peak wave period, peak phase speed, wave angle and steepness. All together, 18 cases are reported. The maximum and minimum wavelengths in this dataset are 75.8 and 28.6 m.

Janssen (1997) carries out a statistical error analysis of the HEXMAX data to investigate the sea-state influence on wind-stress. The HEXMAX data are collected from a research platform at a nominal depth of 18 m. The wind stress is calculated by the eddy correlation method. The dataset (58 cases) has been carefully screened to remove unsteady events and swell-contaminated cases. The wind stress, wind speed at 10 m elevation, peak phase speed and significant wave height are tabulated. The characteristic wavelength needed for the present analysis is derived by the dispersion relation using the tabulated phase speed and the nominal water depth. The maximum and minimum wavelengths in this dataset are 101.6 and 53.4 m.

Figure A1 shows several presentations of C_{10}, including (a) $C_{10}(U_{10})$, (b) $C_{10}(\omega_{**})$, and (c) $C_{10}(U_{10}/C_p)$. The dimensionally consistent expressions (Figs. A1(b) and (c)) reveal the stratification of C_{10} with wavelength. The wavelength ranges of the four datasets are (101.6 m, 53.4 m) in Janssen (1997), (75.8 m, 28.6 m) in Anctil and Donelan (1996), (19.0 m, 8.6 m) in Merzi and Graf (1985), and (5.7 m, 3.3 m) in Donelan (1979). For dimensionally inconsistent expression such as $C_{10}(U_{10})$ shown in Fig. A1(a), such a wave effect is still discernable. The results shown in Fig. A1 suggest that the drag coefficient in terms of C_{10} cannot be expressed as a single-parameter function. Two-parameter functions, such as $C_{10}(U_{10}, u_*/C_p)$ and $C_{10}(U_{10}, U_{10}/C_p)$ have been reported.

Appendix B. A Comparison of $C_{\lambda/2}$ and $C_{\lambda/n}$

The drag coefficient, being the square of the ratio between the wind friction velocity and a reference wind speed, is quantitatively affected by the choice of the reference wind speed. It is demonstrated in Figs. 1 and A1 that the same group of data can be better organized when presented in terms of $C_{\lambda/2}$ in comparison with C_{10}. If an elevation other than one-half of the wavelength is used for the vertical length scale, the equation of the drag coefficient can be written as

$$C_{\alpha/k} = \kappa^2 \left(\ln \frac{\alpha}{k_p z_0} \right)^{-2}, \qquad \text{(B1)}$$

where $k_p = 2\pi/\lambda$. The drag coefficient $C_{\lambda/2}(\omega_{**})$, $C_{\lambda/4}(\omega_{**})$, $C_{\lambda/6}(\omega_{**})$, and $C_{\lambda/8}(\omega_{**})$ of the assembled data are displayed in Fig. B1. As expected, the collapsing of measurements is not influenced by the choice of the proportionality constant for wavelength scaling.

References

Anctil, F. and M. A. Donelan (1996): Air-water momentum flux observed over shoaling waves. *J. Phys. Oceanogr.*, **26**, 1344–1353.

Charnock, H. (1955): Wind stress on a water surface. *Quart. J. Roy. Meteor. Soc.*, **81**, 639.

Donelan, M. A. (1979): On the fraction of wind momentum retained by waves. p. 141–159. In *Marine Forecasting*, ed. by J. C. J. Nihoul, Elsevier.

Donelan, M. A. (1982): The dependence of the aerodynamic drag coefficient on wave parameters. *Proc. First Int. Conf. on Meteorol. and Air-Sea Interaction of the Coastal Zone*, The Hague, Amer. Meteor. Soc., Boston, MA, 381–387.

Donelan, M. A. (1990): Air-sea interactions. p. 239–292. In *The Sea: Ocean Engineering Science*, ed. by B. LeMéhauté and D. M. Hanes, John Wiley & Sons, Inc.

Donelan, M. A., F. W. Dobson, S. D. Smith and R. J. Anderson (1993): On the dependence of sea surface roughness on wave development. *J. Phys. Oceanogr.*, **23**, 2143–2149.

Garratt, J. R. (1977): Review of drag coefficients over oceans and continents. *Mon. Wea. Rev.*, **105**, 915–929.

Geernaert, G. L. (ed.) (1999): *Air-Sea Exchange: Physic, Chemistry and Dynamics*. Kluwer Academic Publ., Dordrecht, The Netherlands, 578 pp.

Janssen, J. A. M. (1997): Does wind stress depend on sea-state or not?—A statistical error analysis of HEXMAX data. *Bound.-Layer Meteor.*, **83**, 479–503.

Jones, I. S. F. and Y. Toba (eds.) (2001): *Wind Stress over the Ocean*. Cambridge University Press, Cambridge, U.K., 307 pp.

Kitaigorodskii, S. A. (1973): *The Physics of Air-Sea Interaction*. Israel Program for Scientific Translations, Jerusalem (English translation), 237 pp.

Kraus, E. B. (1972): *Atmosphere-Ocean Interaction*. Oxford Univ. Press, Oxford, U.K., 275 pp.

Maat, N., C. Kraan and W. A. Oost (1991): The roughness of wind waves. *Bound.-Layer Meteorol.*, **54**, 89–103.

Makin, V. K. (2003): A note on a parameterization of the sea drag. *Bound.-Layer Meteorol.*, **106**, 593–600.

Makin, V. K. and V. N. Kudryavtsev (1999): Coupled sea surface-atmosphere model. 1. Wind over waves coupling. *J. Geophys. Res.*, **104**, 7613–7623.

Makin, V. K. and V. N. Kudryavtsev (2002): Impact of dominant waves on sea drag. *Bound.-Layer Meteorol.*, **103**, 83–99.

Merzi, N. and W. H. Graf (1985): Evaluation of the drag coefficient considering the effects of mobility of the roughness elements. *Ann. Geophys.*, **3**, 473–478.

Smith, S. D., R. J. Anderson, W. A. Oost, C. Kraan, N. Maat, J. DeCosmo, K. B. Katsaros, K. L. Davidson, K. Bumke, L. Hasse and H. M. Chadwick (1992): Sea surface wind stress and drag coefficients: The HEXOS results. *Bound.-Layer Meteor.*, **60**, 109–142.

Stewart, R. W. (1974): The air-sea momentum exchange. *Bound.-Layer Meteorol.*, **6**, 151–167.

Taylor, P. K. and M. J. Yelland (2001): The dependence of sea surface roughness on the height and steepness of the waves. *J. Phys. Oceanogr.*, **31**, 572–590.

Toba, Y., N. Iida, H. Kawamura, N. Ebuchi and I. S. F. Jones (1990): Wave dependence of sea-surface wind stress. *J. Phys. Oceanogr.*, **20**, 705–721.

Toba, Y., S. D. Smith and N. Ebuchi (2001): Historical drag expressions. p. 35–53. In *Wind Stress over the Ocean*, ed. by I. S. F. Jones and Y. Toba, Cambridge Univ. Press, New York.

Wu, J. (1980): Wind-stress coefficients over sea surface near neutral conditions: A revisit. *J. Phys. Oceanogr.*, **10**, 727–740.